# IMAGING OF PLASMAS USING PROTON BEAMS GENERATED BY ULTRA-INTENSE LASER PULSES

M.Borghesi, D.H.Campbell, R.J.Clarke, M.Galimberti, L.A.Gizzi, M.Haines, A.J.MacKinnon, A.Schiavi, O.Willi*

## INTRODUCTION

During the interaction of ultraintense laser pulses with plasmas and solid targets, a considerable fraction of the laser energy is deposited into highly energetic charged particles. One of the most exciting results recently obtained in this area of research is the observation of very energetic beams of protons, generated during the interaction of ultraintense short pulses with solid targets. In a number of experiments, performed with different laser systems and in different interaction conditions, protons with energies up to several tens of MeV have been detected behind thin foils irradiated with high intensity pulses[1]. In these experiments it was seen that the particle beams are directed along the normal to the back surface of the target, and have a small angular aperture at the highest energies. As proton beams are observed even using target which nominally do not contain hydrogen, protons are thought to originate from hydro-carbon impurities located on the target surfaces[2] or from bulk contamination of the target. Proposed theoretical models indicate that the protons gain their energy from the enormous electric field (~MV/micron) set up by laser accelerated fast electrons via space-charge at the back target surface[3]. As protons are easier to accelerate than heavier ions, protons are the dominant component of the ion emission.

The particular properties of the proton beams (small source size, high degree of collimation, short duration, energy dependence on the target characteristics, ease of synchronization with laser pulses) make them very suitable for application as a probe in dense plasmas investigations. Beside the standard radiographic use, i.e. the detection of aerial density variations[4], proton beams can also be used to detect electric and magnetic

* M.Borghesi, Department of Pure and Applied Physics, the Queen's University of Belfast, Belfast (UK); D.H.Campbell, A.Schiavi, M.G.Haines, Imperial College of Science, Technology and Medicine, London (UK), O.Willi, Institut für Laser- und Plasmaphysik, Heinrich-Heine-Universität, Düsseldorf (Germany), L.A.Gizzi, M.Galimberti, IFAM-CNR, Pisa (Italy), A.J.MacKinnon, Lawrence Livermore National Laboratory, Livermore (CA, USA)

*Advanced Diagnostics for Magnetic and Inertial Fusion*, Edited by Stott *et al.*
Kluwer Academic/Plenum Publishers, New York, 2002

fields generated during the interaction of intense laser pulses with plasmas. In this context, proton imaging can be developed as a diagnostic with great potential for Inertial Confinement Fusion (ICF) studies. For example, the possibility of accessing directly electric field distributions in dense plasmas may shed new light on issues as hydrodynamic and electromagnetic instabilities highly detrimental for ICF. The technique has great potential for access to the complex and yet unexplored electric and magnetic field distributions in indirect drive target assemblies. In a Fast Ignitor context, it can contribute to the study of the large transient electric and magnetic fields generated in high-intensity laser-matter interactions. The magnitude and characteristics of these fields are currently the subject of much conjecture in the short pulse, high-intensity plasma physics community. In this paper the results of an experimental campaign carried out at the Central Laser Facility, Rutherford Appleton Laboratory will be presented and discussed, in which the proton source has been applied for the first time as a particle probe in a range of laser-plasma interaction conditions[5].

## EXPERIMENTAL SET-UP AND DIAGNOSTIC ARRANGEMENT

The VULCAN Nd:glass laser operating in the Chirped Pulse Amplification mode (CPA) was used in the experiment. The main targets (used for the production of the proton beams) were Al foils, 1-2 mm wide and 3 - 25 μm thick. The 1.054 μm CPA interaction pulse, 1 ps in duration, with energy up to 100 J was focused by an F/3.5 off-axis parabola (OAP) onto the centre of the main target. The incidence was about 15° off normal. There was the possibility, exploited in the final part of the experimental campaign, of splitting the main CPA pulse in two separate high-intensity pulses, and to focus them employing two separate F/3.5 Off-Axis Parabolas. The focal spot varied between 8 and 10 μm in diameter at full width at half maximum (FWHM), containing 30-40 % of the energy, and giving intensities up to $5\text{-}7\times10^{19}$ W/cm$^2$. Heating pulses with duration 0.5-1 ns were also available, and were used to provide, in some parts of the experiment, intensities on target in the range $10^{13}$-$10^{15}$ W/cm$^2$. A low-energy fraction of the main CPA pulse was frequency quadrupled and used as a transverse optical probe pulse. A summary description of the beam arrangements used in the various experimental tests performed will be given at the beginning of each experimental section.

The detector employed in the whole campaign consisted of a stack of several layers of radiochromic (RC) film. The film consists of 270 μm thick plastic containing a double layer of organic dye, which reacts to ionizing radiation[6]. The equivalent dose of energetic protons stopped in the film can be measured from the changes in optical density undergone by the film, yielding information on the number and energy of the protons. By using them in a stack, each layer of film acts as a filter for the following layers. Since protons deposit energy mainly in the Bragg peak at the end of their range, each RC film layer spectrally selects a narrow range of proton energies. 25-50 μm Al filters were placed in front of the first layer of film giving a minimum detectable proton energy of about 3 MeV.

The laser-produced proton beam was characterized in view of its application as a particle beam probe. The protons were produced by focusing the CPA pulse onto the Al

foil, and detected by placing the RC film stack at the back of the target, typically at a distance of about 2 cm. It was found that the proton beams have high brightness, typically with $10^{12}$ protons with energy above 3 MeV per shot (at a laser irradiance of the order of 5 $10^{19}$ $Wcm^{-2}$). As observed in previous experiments, the beams were highly directional, propagating along the normal to the back surface of the target with small angular divergence (about 15° for 10 MeV protons). The response of each RCF layer to high-energy protons has been determined using Monte Carlo modelling of the deposited energy by the particles[7]. Each film shown responds to ions within an energy band of less than 1MeV. For I ~5-7 $10^{19}$ $W/cm^2$ a strong proton signal was observed out to the layer corresponding to proton energy just above 20MeV. The energy deposited within each film layer can be extracted from the absolutely calibrated film. By doing this for each film layer and fitting an exponential energy spectrum, an estimate of the proton energy spectrum and total energy could be extracted from the film data[7]. The mean proton energy of the exponential fit is 3.75MeV ± 0.3MeV with a total energy of 2.2J in an equivalent Maxwellian with a temperature of 2.5MeV. During the experiments the source size of the proton beam was estimated using a penumbral edge method, setting an upper limit of 15-20 μm diameter for the source of 10 MeV protons (there is debate if this is the real or just the apparent source size).

The main reasons making laser-produced proton beams particularly interesting for probing applications are: the small source size, leading to high spatial resolution in imaging applications; the short pulse duration, measured to be a few ps in our conditions; the low divergence and high brightness of the beam; the long stopping range of 10-30 MeV protons, i.e. the possibility of penetrating reasonably thick objects. In addition, high spatial and spectral resolution is guaranteed by an appropriate choice of detector (e.g. RCF stacks), and the proton beam characteristics can be tuned by suitably changing the laser and target parameters. The temporal resolution obtainable with these beams is far beyond the possibilities of beams provided by conventional accelerators. Further, as it will be seen in the following sections, the fact that the beams are not monochromatic is far from being a disadvantage for the proposed applications. Finally their ease of use and synchronization is a clear advantage in laser-plasma and Inertial Confinement-Fusion related experiments.

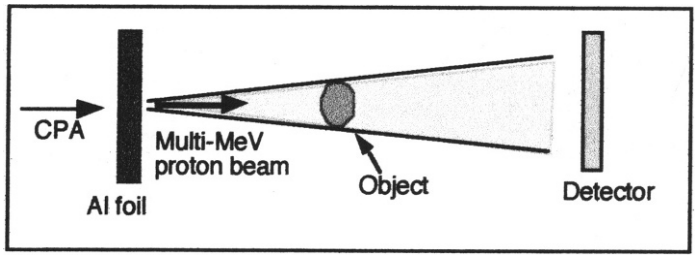


**Figure 1** - Schematic arrangement for proton imaging.

Thanks to the small size of the source, we were able to implement a scheme of point projection imaging, with the object placed between the proton source (i.e. the back side of the primary target) and the detector (see fig. 1). The magnification of the image was determined by the ratio of the detector-to-object and object-to-source distances

## IMAGING OF THIN CHARGED OBJECTS

When thick solid obstacles were placed in the beam a shadow of the object was observed in the proton beam, due to collisional stopping in the target. However, a shadow was observed even when objects with a thickness much smaller than the proton penetration depth were used, e.g. meshes formed by 10 μm Cu wires with 25 μm spacing, or by 25 μm Cu wires with 100 μm spacing. The meshes were parallel to the main target, i.e. perpendicular to the proton beam. The distance between the proton source and the mesh was 1 mm, while the first of the radiochromic film layers was positioned at 22 mm from the source.

A shadow of the mesh was observed on the radiochromic film, as shown in fig. 2(a). The image shown in the picture has been obtained with 15 MeV protons and the 25 μm spacing mesh. Fig.2(b) shows the optical density lineout across the shadow of a mesh with 100 μm spacing, obtained with 20 MeV protons. The optical density modulation observed is of the order of 0.2. It should be reminded that the stopping range of 20 MeV protons in Cu is about 800 μm, and the collisional energy loss for such energetic protons in 25 μm of Cu is just $\Delta E/E \sim 2\ 10^{-4}$. Such a variation is too small to produce any detectable effect on our diagnostic. Under these conditions scattering is also unimportant, therefore the shadow observed must be due to some different effect. Our present explanation is that the mesh charges up positively, due, for example, to hot electrons preceding the proton beam and expelling cold electrons from the target.

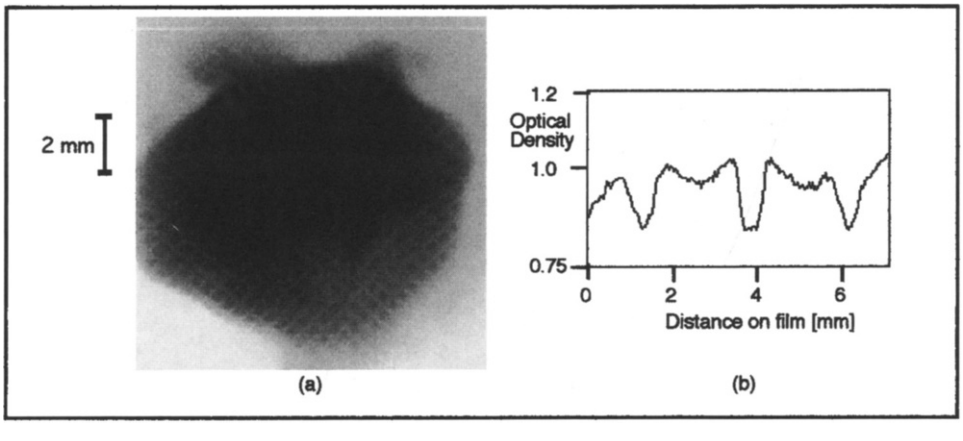


**Figure 2** - (a) Image of a mesh with 25 μm spacing (10 μm Cu wires) obtained with 15 MeV protons; (b) Lineout across image of a mesh with 100 μm spacing (25 μm Cu wires) obtained with 20 MeV protons.

The deflection of the protons due to the electric field in the proximity of the wires is then responsible for the creation of the mesh shadow on the detector, where pile-up of the deflected protons is observed beside the regions of minimum transmission. An estimate of the linear charge $\lambda$ on the mesh can be obtained via particle tracing, giving $\lambda \sim 10^{-6}$ C/m.

## IMAGING OF LASER-PRODUCED PLASMAS

The sensitivity of the proton beam to electric fields, demonstrated in the measurements reported in the previous section, makes proton imaging a valid and unique diagnostic for investigating electric field distributions inside plasmas. The diagnostic potential of this application was tested in part of our experimental campaign. A preformed plasma was created by irradiating a secondary target with 600 ps, 0.527 μm heating pulses, prior to the CPA pulse interaction with the primary target. Both *face-on* (proton propagation axis parallel to the main plasma axis) and *side-on* (proton propagation axis perpendicular to the main plasma axis) geometry was used.

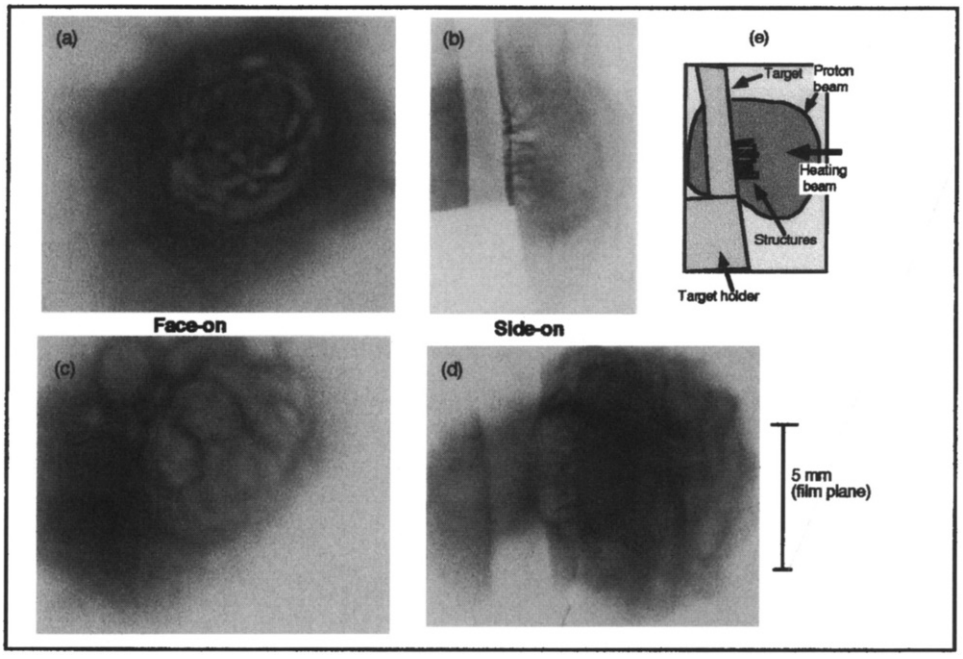


**Figure 3** - Face-on and side-on proton images of plasmas produced by laser irradiation of 25 $\mu$m foils: (a),(b): Heating focal spot : 100 $\mu$m diameter with no beam smoothing, irradiance: I ~ 5 $10^{14}$ W/cm$^2$; (c), (d) Heating focal spot: 250 $\mu$m diameter with beam smoothing (Phase Zone Plates) I~ $10^{14}$ W/cm$^2$. (e) Schematic showing the main characteristics of the side-on images.

The proton beam was produced as usual from a 25 μm Al foil, and the secondary target also consisted of a 25 μm Al foil. The heating irradiance on target varied between 5 $10^{13}$ and $10^{15}$ W/cm2, with typical delays between the plasma formation and the CPA interaction with the primary target in the range 200-800 ps. When no preformed plasma was produced onto the secondary Al foil, the proton beam was, as expected, unperturbed, except for some charging-up-induced deflection at the edge of the foil. When the secondary foil was laser-heated the situation changed, and, under certain conditions, the presence of the plasma perturbed significantly the intensity distribution of the proton beam. Most importantly the perturbations imposed on the intensity profile of the proton beam appeared to depend strongly on the plasma conditions.

As a matter of fact, changing the irradiation parameters led to striking differences in the modulation pattern superimposed onto the proton beam. An example of this is given in fig. 3, where the RC film images pertaining to different irradiation conditions are shown. The structures observed differ markedly between the case in which no beam smoothing is applied to the beam, and the case in which Phase Zone Plates (PZP)[8], producing an ordered hot spot structure in the focal spot profile, are employed. In particular side-on images indicate clearly the presence of chaotic structures in the former case, while a regular pattern is observed in the latter. In all cases these structures were only observed within the duration of the heating pulse, and disappeared at later times. We believe that these structures are caused by electric fields present inside the plasma, which are strictly related to the laser intensity distribution. Detailed analysis and modelling is undergoing.

## IMAGING OF ULTRAINTENSE INTERACTIONS

In part of the experimental campaign, proton imaging was applied to the study of ultraintense laser-plasma interactions. These measurements took advantage of the unique possibility of employing two temporally and spatially independent high-power CPA pulses. The second pulse ($CPA_2$) was split off the main pulse ($CPA_1$) before amplification. Due to set-up constrains, the energy content of each pulse was about 20 J, focusable to intensities in the range 0.5-1.0 $10^{19}$ W/cm$^2$. The temporal separation of the two pulses could be varied shot-to-shot. The two beams were focused from different directions with separate f/3.5 optics. The $CPA_2$ pulse was used to produce a proton beam from an Al foil, and the proton beam was used to probe, transversely, the interaction of the $CPA_1$ pulse with solid targets.

It should be noted here that, when probing an object undergoing fast changes, the fact that the proton beams are not monochromatic is actually an advantage, as it can be exploited to obtain, in a single shot, information on the temporal history of the object to be probed. In fact, if the object to be probed is situated at a finite distance from the source, protons with different energies will reach the object at different times. By employing a detector that performs spectral selection, the information on the temporal evolution of the target can be retained. In particular, proton imaging was employed to observe the fast evolution of the electric fields following the irradiation of solid targets (wires, foils and micro-balloons) with the $CPA_1$ pulse.

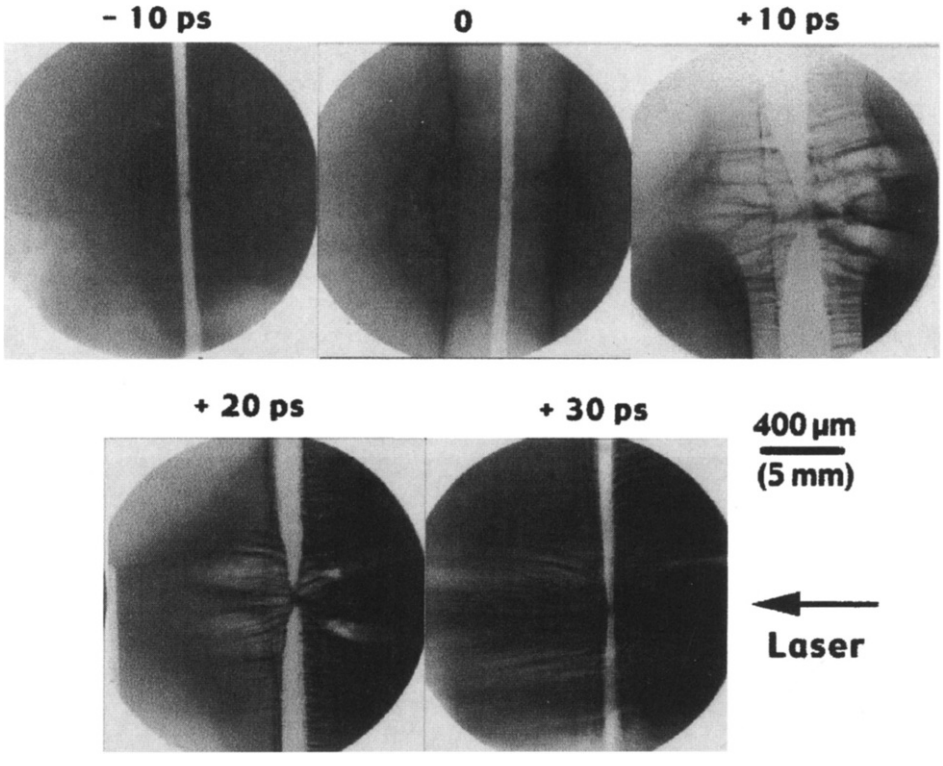


**Figure 4** - Temporal evolution of proton images of the interaction zone for different interaction-probing delays. The target was a 50 $\mu$m Ta wire and the energy of the protons employed was 6-7 MeV. The delay between $CPA_1$ interaction and probing is indicated above each of the pictures. Spatial scales for both the target and the image plane (between bracket) are indicated.

Particularly dramatic effects were observed probing the interaction of the $CPA_1$ pulse with small diameter metal wires. Fig.4 shows proton images of the interaction with a 50 $\mu$m Ta wire. The RCF layers shown (second layers of the RCF stacks, corresponding to proton energies of 6-7 MeV) have been obtained in separate shots for different $CPA_1$-$CPA_2$ delays. When the proton probe arrived on target before the $CPA_2$ interaction pulse (e.g., t=-10 ps, first image in fig.4), the shadow of the Ta wire, thick enough to slow down the protons can be seen, with some small effect visible in the interaction region due to preplasma present ahead of the interaction. However when the probe is coincident with the interaction a dramatic effect is observed, with the protons being deflected away from the wire surface, which charges up due to hot electron expulsion. The charge is seen to decay in a few tens of picoseconds, as filamentary structures (horizontal striations) are seen to appear. The appearance of these structures is consistent with the growth, at the surface of the target, of an electromagnetic heat-flow instability, such as for example the electro-thermal instability[9].

The instability causes filamentation of the hot current, and as the filaments are magnetized, the effect is imprinted on the proton beam via the radial electric fields present inside the filaments. The onset of pronounced symmetrical horizontal features above and below the interaction axis is also detected. Such structures may be related to the radial expansion of shocks following the interaction, likely presenting non-neutral regions at their leading front.

## CONCLUSION

Proton imaging is a diagnostic with enormous potential for the investigation of fundamental plasma physics problems which were impossible to explore up to now. By using this diagnostic, for the first time the measurement of transient electric fields in dense plasmas has been obtained, determining their evolution on a picosecond scale with micrometric spatial resolution. The data is of great relevance to Inertial Confinement Fusion both in the conventional and Fast Ignitor approach. Detailed analysis and modelling is presently undergoing.

## ACKNOWLEDGEMENT

The work was supported by an ESPRC grant. We acknowledge the invaluable contribution to the work provided by the Central Laser Facility staff at the Rutherford Appleton Laboratory, and fruitful discussions with Dr. H.Ruhl (General Atomics).

## REFERENCES

1. E.L Clark *et al*, Measurements of energetic proton transport through magnetized plasma from intense laser interactions with solids, Phys. Rev. Lett. **84**, 670 (2000); R.D.Snavely *et al*, Intense high-energy proton beams from Petawatt-laser irradiation of solids, Phys. Rev. Lett., **85**, 2945 (2000)

2. S.J.Gitomer *et al*, Fast ions and hot electrons in the laser-plasma interaction, Phys. Fluids **29**, 2679 (1984)

3. S. Wilks *et al*, Energetic proton generation in ultra-intense laser--solid interactions, Phys.Plasmas **8**, 542 (2001); A.Pukhov, Three-dimensional simulations of ion acceleration from a foil irradiated by a short-pulse laser, Phys. Rev. Lett, **86**, 3562 (2001); H.Ruhl *et al*, Computer simulation of the three-dimensional regime of proton acceleration in the interaction of laser radiation with a thin spherical target, Plasma Phys. Rep. **27**, 363 (2001)

4. J.A. Cookson, Radiography with protons, Naturwissenschaften, **61** 184 (1974)

5. M.Borghesi *et al*, Proton imaging: a diagnostic for Inertial Confinement Fusion/Fast Ignitor studies, to be published in Plasma Phys. Control. Fusion (2001)

6. W.L.C. McLaughlin *et al*, Sensitometry of the response of a new radiochromic film dosimeter to gamma radiations and electron beams, Nucl. Instr. Methods Phys. Res. A, **302**, 165 (1991)

7. A.J.Mackinnon *et al*, Effect of plasma scale length on multi-MeV proton production by intense laser pulses, Phys. Rev. Lett., **86**, 1769 (2001)

8. T.H.Bett *et al*, Binary phase zone-plate arrays for laser-beam spatial-intensity distribution conversion, Appl. Opt., **34**, 4025 (1995)

9. M.G.Haines, Thermal instability and magnetic field generated by large heat-flow in a plasma, especially under laser-fusion conditions, Phys. Rev. Lett. **47**, 918 (1981)